ISSN 1009 – 3095 *Journal of Zhejiang University SCIENCE* V.4, No.2, P.202 – 206, Mar. – Apr., 2003
http://www.periodicals.com.cn; http://www.zju.edu.cn/English

http://www.zjupress.com; http://lib.zju.edu.cn/eindex.htm; jzus@zju.edu.cn

Shape optimization of plate with static and dynamic constraints via virtual laminated element*

LI Fang (李芳)[1,2†], XU Xing(徐兴)[1], LING Dao-sheng(凌道盛)[1]

([1] *Department of Civil Engineering, Zhejiang University, Hangzhou 310027, China*)

([2] *College of Electromechanical Engineering, Zhejiang University of Technology, Hangzhou 310032, China*)

†E-mail: lif1110@163.com

Received Mar.28, 2002; revision accepted June.29, 2002

Abstract: The virtual laminated element method (VLEM) can resolve structural shape optimization problems with a new method. According to the characteristics of VLEM, only some characterized layer thickness values need be defined as design variables instead of boundary node coordinates or some other parameters determining the system boundary. One of the important features of this method is that it is not necessary to regenerate the FE(finite element) grid during the optimization process so as to avoid optimization failures resulting from some distortion grid elements. The thickness distribution in thin plate optimization problems in other studies before is of stepped shape. However, in this paper, a continuous thickness distribution can be obtained after optimization using VLEM, and is more reasonable. Furthermore, an approximate reanalysis method named "behavior model technique" can be used to reduce the amount of structural reanalysis. Some typical examples are offered to prove the effectiveness and practicality of the proposed method.

Key words: Optimum design, Virtual laminated element method(VLEM), Behavior model technique, Structural reanalysis

Document code: A **CLC number:** O224

INTRODUCTION

In structural design, it is necessary to find the appropriate configuration of a structure subjected to given loads. Configuration of a structure includes parameters such as its dimension, its shape, its topology and so on. The object of optimization often requires that a structure must have a minimum in weight, reach the maximum in its strength and stiffness, and reasonable values in natural frequencies within a specified design domain.

Shape optimization is much more complicated than dimension optimization, because the boundary shape is continuously changing in the optimization design processes so that the description of boundary shape changes must be taken into account. Meanwhile we should maintain proper finite element grid accuracy, thus ensuring sensitivity analysis and proper constraint setting.

When coordinates of boundary nodes of finite elements are used as design variables (Zienkiewicz et al., 1973), some distortion finite elements possibly can lead to failure of optimization results. Using high order polynomial functions to describe boundary shape can cause the boundary to be oscillatory. Thus a modification method is introduced through using spline combined with low order polynomial terms, to describe the boundary shape (Imam, 1982; Sienz et al., 1997).

However, VLEM provides shape optimization with a new method.

VIRTUAL LAMINATED ELEMENT

The virtual laminated element method (VLEM) can be easily applied to laminated composite material structure problems, The effectiveness of VLEM when applied to engineering can be found in references (Wu, 1997; Ling et al., 1998; Xu et al., 2001). The basic idea of VLEM lies in the introduction of the concept of virtual lamina. The virtual lamina does not contain any real material at all; elasticity tensor E

* Project (No.50075083) supported by National Natural Science Foundation of China

can be zeroed, i.e. the lamina is an empty one. Normal elements could be constructed through setting up an empty lamina among laminae so that the same element can be made up of different materials. Through iso-parametric element transformation, any finite element nodes in global coordinate system could be defined anywhere in a real structure, either at its boundary, inside it, or outside it.

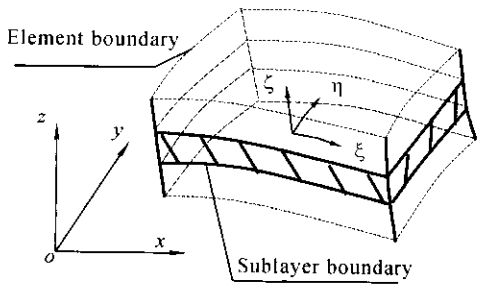

Fig.1 Virtual laminated element

1. 3D-degenerated solid plate-shell element

The 16-noded plate-shell element shown in Fig. 2 was degenerated from a 20-noded 3D brick. Here it is used to construct virtual laminated plate-shell element.

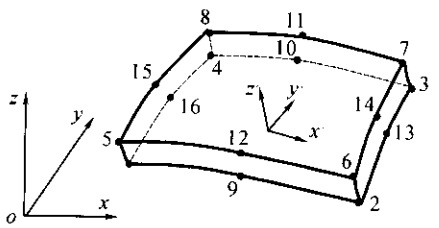

Fig. 2 16-noded plate-shell element degenerated from 20-noded 3D brick

In Fig. 1, parent element boundaries are characterized by ξ, η, *and* $\zeta = \pm 1$. $\zeta = -1$ represents the bottom side of the virtual laminated plate-shell , and $\zeta = +1$ means the top side of it. It can be divided into n sublayers between the sides of $\zeta = -1$ and $\zeta = +1$. Coordinate ζ for each of them is marked by $\zeta_0, \zeta_1, \ldots \zeta_n$, respectively. Here suppose $n = 3$.

Coordinate system transformation between the element and parent element is

$$\begin{Bmatrix} x \\ y \\ z \end{Bmatrix} = \sum_{i=1}^{16} N_i(\xi, \eta, \zeta) \begin{Bmatrix} x_i \\ y_i \\ z_i \end{Bmatrix}, \qquad (1)$$

where x_i, y_i, z_i are global ordinates of element nodes. The form function N_i is the same as that of 3D solid isoparameter element, i.e.

$$N_i = \frac{1}{8}(1 + \xi\xi_i)(1 + \eta\eta_i)(1 + \xi\xi_i)(\xi\xi_i + \eta\eta_i + \zeta\zeta_i - 2) \quad (i = 1, 2, \cdots, 8)$$

$$N_i = \frac{1}{4}(1 - \xi^2)(1 + \eta\eta_i)(1 + \zeta\zeta_i) \quad (i = 9, 10, 11, 12)$$

$$N_i = \frac{1}{4}(1 - \eta^2)(1 + \xi\xi_i)(1 + \zeta\zeta_i) \quad (i = 13, 14, 15, 16)$$

In Fig. 2, local coordinate system $x'y'z'$ is set up to introduce some plate-shell basic hypotheses. z' is directed along the normal direction of element surface, and x' and y' lie on the element surface plane.

To construct 3D-degenerated solid plate-shell element from 3D brick, we need to introduce the following plate-shell basic hypotheses:

(1) Normam stresses along the direction of plate-shell thickness can be omitted, i.e. $\sigma_{z'} = 0$.

(2) $\sigma_{z'} = 0$ makes $\varepsilon_{z'}$ not be independent, consequently the relative deflection $\Delta w'$ between the top and bottom sides of the element will also become not independent and be constrained away. For $\Delta w'$ being a minor one, set the constraints

$$\Delta w' = 0 \quad (i = 1, 2, \cdots, 8)$$

Therefore, the degree of freedom of the element will be reduced from 48 to 40.

2. Laminated plate-shell element stiffness matrix

Because the material elastic modulus matrix $\boldsymbol{D}_k$ is different in each sublayer, an element stiffness matrix is established by being integrated on each sublayer as follows:

$$k_{ij} = \sum_{k=1}^{n} \int_{\zeta_{k-1}}^{\zeta} \int_{-1}^{1} \int_{-1}^{1} \boldsymbol{B}_i^{\mathrm{T}} \boldsymbol{D}_k \boldsymbol{B}_j \mid \boldsymbol{J}_k \mid \mathrm{d}\xi \mathrm{d}\eta \mathrm{d}\zeta \qquad (2)$$

For Gauss integration on each sublayer, Eq. (2) was changed by the following transformation:

$$\zeta = \sum_{i=1}^{16} N_i(\xi', \eta', \zeta')\zeta_i; \quad \xi = \xi'; \quad \eta = \eta'$$

Substituting it into Eq.(2) yields:

$$k_{ij} = \sum_{k=1}^{n} \int_{-1}^{1} \int_{-1}^{1} \int_{-1}^{1} \boldsymbol{B}_i^{\mathrm{T}} \boldsymbol{D}_k \boldsymbol{B}_j \mid \boldsymbol{J}_k \mid \mid \boldsymbol{J}_k' \mid \cdot$$

$$d\xi' d\eta' d\zeta' \tag{3}$$

where

$$|\boldsymbol{J}_k'| = \begin{vmatrix} \frac{\partial \xi}{\partial \xi'} & \frac{\partial \xi}{\partial \eta'} & \frac{\partial \xi}{\partial \zeta'} \\ \frac{\partial \eta}{\partial \xi'} & \frac{\partial \eta}{\partial \eta'} & \frac{\partial \eta}{\partial \zeta'} \\ \frac{\partial \zeta}{\partial \xi'} & \frac{\partial \zeta}{\partial \eta'} & \frac{\partial \zeta}{\partial \zeta'} \end{vmatrix} = \begin{vmatrix} 1 & 0 & 0 \\ 0 & 1 & 0 \\ \frac{\partial \zeta}{\partial \xi'} & \frac{\partial \zeta}{\partial \eta'} & \frac{\partial \zeta}{\partial \zeta'} \end{vmatrix} = \frac{\partial \zeta}{\partial \zeta'}$$

Eq. (3) then becomes:

$$k_{ij} = \sum_{k=1}^{n} \int_{-1}^{1}\int_{-1}^{1}\int_{-1}^{1} \boldsymbol{B}_i^{\mathrm{T}} \boldsymbol{D}_k \boldsymbol{B}_j \, |\boldsymbol{J}_k| \cdot \frac{\partial \zeta}{\partial \zeta'} d\xi' d\eta' d\zeta' \tag{4}$$

Corresponding the isotropy linear-elastic material in the layer, the modulus matrixis $\boldsymbol{D}_k$ is(It can be kept unified in form by introducing penalty factor λ)

$$\boldsymbol{D}_k = \frac{E}{1-\mu^2} \begin{bmatrix} 1 & & & & & \\ \mu & 1 & & & \text{symmetry} & \\ 0 & 0 & \lambda & & & \\ 0 & 0 & 0 & \frac{1-\mu}{2} & & \\ 0 & 0 & 0 & 0 & \frac{1-\mu}{2} & \\ 0 & 0 & 0 & 0 & 0 & \frac{1-\mu}{2} \end{bmatrix}$$

A penalty factor is introduced into the material elastic matrix $\boldsymbol{D}_k$ so that λ can be zeroed in the case of calculating stresses on the basis of strains so as to satisfy plate-shell basic hypothesis Eq.(1), and D_k will be given a large value which makes $\varepsilon_{z'}$ tend to zero when composing the element stiffness matrix to satisfy the plate-shell basic hypothesis Eq.(2).

PROBLEM FORMULATION AND OPTIMIZATION METHOD

A shape optimization problem can be mathematically generalized as follows:

$$\text{Minimize} \quad F(\boldsymbol{x}) \tag{5a}$$

$$\text{Subject to} \quad g_j(\boldsymbol{x}) \geqslant 0 \quad j = 1, 2, \cdots, m \tag{5b}$$

$$x_{\min} \leqslant x_i \leqslant x_{\max} \quad i = 1, 2, \cdots, n \tag{5c}$$

Where $\boldsymbol{x} = [x_1 \quad x_2 \quad \cdots \quad x_n]^{\mathrm{T}}$; $F(\boldsymbol{x})$ is objective function; $g_j(\boldsymbol{x})$ are constraint functions. In this paper, objective functions Eq. (5a) are the minimum weights of a structure. The behavior constraints Eq. (5b) are those of stresses, displacements, and natural frequencies of a structure. The geometric constraints Eq. (5c) mean those of a structure's dimensional deformation domain.

Objective and constraint functions can be approximately expressed by a quadratic Taylor series which, compared to linear expansion, requires a greater number of finite element analyses. The quadratic expansion is written as:

$$f(\boldsymbol{x}) = f(\boldsymbol{x}_k) + \nabla f(\boldsymbol{x}_k)(\boldsymbol{x} - \boldsymbol{x}_k) + \frac{1}{2}(\boldsymbol{x} - \boldsymbol{x}_k)^{\mathrm{T}} \boldsymbol{H}(\boldsymbol{x}_k)(\boldsymbol{x} - \boldsymbol{x}_k) \tag{6}$$

Where $\boldsymbol{x}_k = [x_{k1} \quad x_{k2} \quad \cdots \quad x_{kn}]^{\mathrm{T}}$. They are the initial design points for each cycle or responding surface. $\nabla f(\boldsymbol{x}_k)$ are gradients of the objective or constraint functions. To reduce the number of finite element analysis, $\boldsymbol{H}(\boldsymbol{x}_k)$ is taken as the Hessian matrix just with diagonal terms (without cross-coupling terms). This method is called "behavior model technique".

Once quadratic Eq. (6) approximate functions have been generated, they can be used to determine the values of objective and constraint functions at optimization points on each responding surface during the optimization processes.

By means of Sequential Unconstrained Minimization Technique (SUMT), Eqs. (5a-5c) can be transformed into

$$P(\boldsymbol{x}, \boldsymbol{r}_k) = F(\boldsymbol{x}) + r_k^{-1} \sum_{j=1}^{m} \{\min[0, g_j(\boldsymbol{x})]\}^2 \quad k = 1, 2, \cdots \tag{7}$$

Different penalty factor r_k often form different corresponding penalty function $P(\boldsymbol{x}, \boldsymbol{r}_k)$, with each $P(\boldsymbol{x}, \boldsymbol{r}_k)$ describing a responding surface, so $P(\boldsymbol{x}, \boldsymbol{r}_k)$ are called responding functions.

FEM analyses can be carried out using each perturbation to design points on each responding surface so as to generate quadratic Eq. (6) approximate functions. For each response surface, we can get optimum design points with the Newton method during the search for an optimum for

unconstrained optimization Eq. (7).

RESULTS

To show the effectiveness of the method developed herein on shape optimization, one dynamic problem and two static problems are presented below.

1. Thickness optimization of a simply supported square plate with deflection constraints

The first example is to find the minimum weight of a simply supported square plate with deflection constraints shown in Fig.2. It is subjected to a concentrated load of 40 KN at its center where the maximum admissible deflection is 0.02 m. The material properties are as follows: $E = 2.1 \times 10^5$ MPa, $\nu = 0.3$, $\rho = 7800$ kg/m^3. The dimensions of the plate are assumed to be 10 m × 10 m. The minimum admissible thickness after optimization is set to be 0.005 m.

Using its symmetry characteristics permits the analysis to be conducted on only a quarter of the plate, which was divided into 16 3D-virtual laminated plate elements. The thickness at corner nodes of the solid layer is taken as the design variable (Fig. 3); the number of which is as many as 25. Table 1 and Fig.5. show the final design results.

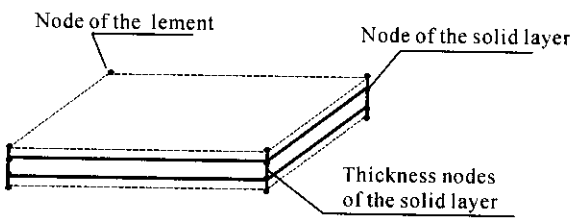

Fig.3 Thickness optimization at the corner nodes of the element

Fig.4 Plate section of stepped shape

Table 1 Comparison of the final data with deflection constraint

	Weight (kg)	Deflection(mm)
(Fleury et al., 1983)	7180	19.89
(Kang et al., 1986)	6960	< 20.00
Method presented	6599	19.80

It is worth pointing out that the introduction of VLEM here makes thickness in the same element be different so that the obtained thickness

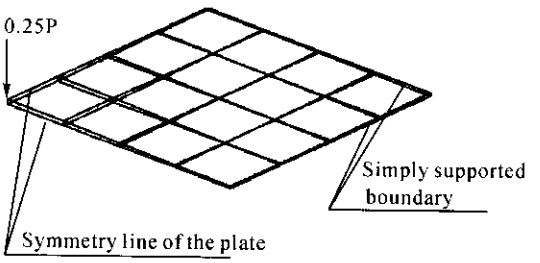

Fig.5 Thickness distribution of the plate after optimization with deflection constraints

distribution of the thin plate after optimization becomes more reasonable than that of the stepped shape (Fig. 4) in other researches (Fleury et al., 1983; Ramana et al., 1993). Fig.6 shows the resulting thickness values of solid layers at element nodes after optimization using virtual laminated element.

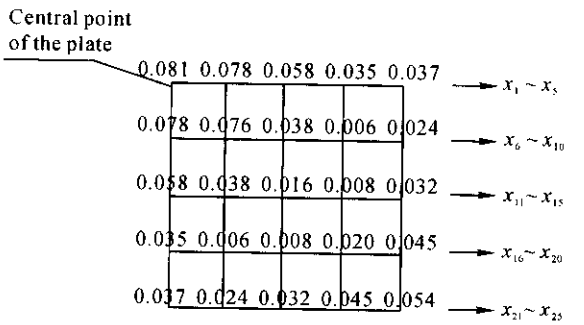

Fig.6 Thickness data distribution of the plate after optimization with deflection constraints(dimensions in millimeters)

2. Thickness optimization of simply supported square plate with frequency constraints

The second example is concerned with the minimum weight design of a plate subjected to a natural frequency constraint. The dimensions of the plate are 25.4 cm × 25.4 cm, and its assumed material properties are: $E = 2.1 \times 10^5$ MPa, $\nu = 0.3$, $\rho = 7800$ kg/m^3, and under the constraints of both admissible minimum fundamental frequency assumed to be $f = 11.2$ Hz and admissible minimum thickness values (T_{min}) – 0.254 cm, 0.127 cm and 2.54×10^{-3} cm respectively. To find the minimum weight of the plate (the example cited from Fleury et al.(1983) in British units of its origin, was changed here into metric system). The initial design corresponding to a uniform thickness $a^0 = 0.305$ cm.

Table 2 Comparison of the final data with frequency constraint

	$T_{min}=0.254$cm		$T_{min}=0.127$cm		$T_{min}=2.54\times10^{-3}$cm	
	weight (kg)	frequency(Hz)	weight (kg)	frequency(Hz)	weight (kg)	frequency(Hz)
(Fleury et al., 1983)	0.341	11.20	0.262	11.30	0.236	11.30
Method developed herein	0.343	11.20	0.261	11.24	0.226	12.10

The finite element grid remains the same as that of the first example. Table 2 and Fig. 7 show the final design results. When the admissible minimum thickness became small, the weight of the plate we obtained became even smaller. Fig. 7 shows the 3D structural schematic diagram of the plate in one of the above three cases with a constraint of admissible minimum thickness to be 2.54×10^{-3} cm . The other two cases yielded similar results.

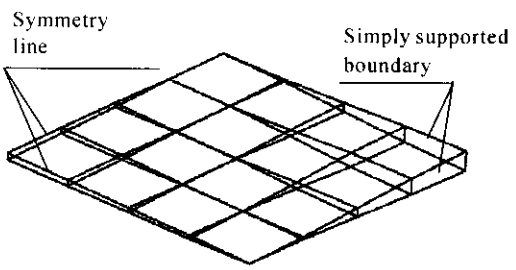

Fig.7 Thickness distribution of the plate after optimization with frequency constraints

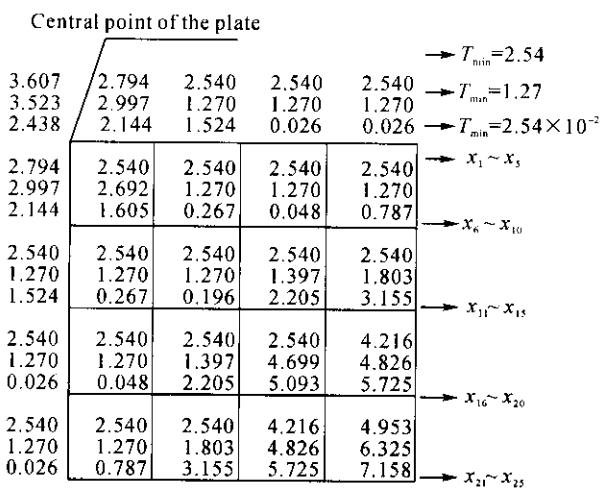

Fig.8 Thickness data distribution of the plate after optimization with frequency constraints (dimensions in millimeters)

The above results show that if the weight of a plate does not change, distributing more material over both near center locations and near corners can raise the minimum fundamental frequency of the plate.

CONCLUSIONS

1. The virtual laminated element method (VELM) achieves shape optimization with a new method. According to the characteristics of this element, the original FE data structure need not be changed, i.e. there is no need to regenerate FE grid.

2. Using "behavior model technique" with the linear and diagonal terms in the Hessian matrix can fully resolve nonlinear optimization problems with adequate accuracy. Also, the technique can substantially reduce the number of finite element reanalyses required.

3. In this paper, the initial penalty factor is assumed to be 1.0, and decay factor to be 0.25. Generally, calculation can achieve convergence after going through 5 – 8 responding surfaces.

References

Fleury, C. and Sander, G., 1983. Dual methods for optimizing finite element flexural systems. *Computer Methods in Applied Mechanics and Engineering*, **37**(3): 249 – 275.

Imam, M. H., 1982. Three-dimensional shape optimization. *Int J Numer Meth Engng*, **18**: 661 – 673.

Kang, J.Z., Ye, D.Y., 1986. A feasible direction method for the optimum design of thin plate. *Computational Structural Mechanics and Applications*, **3**(3): 67 – 76 (in Chinese).

Ling, D.S., Zhang, J.J., Xiang, Y.Q. and Xu, X., 1998. The method of virtual laminated element and its application in bridge engineering . *China Civil Engineering Journal*, **31**(3): 22 – 29 (in Chinese).

Ramana, V., Grandhi and Geetha Bharatram, 1993. Multiobjective optimization of large-scale structures. *AIAA Journal*, 1993, **31**(7), 1329 – 1337

Sienz, J. and Hinton, E., 1997. Reliable structural optimization with error estimation, adaptivity and robust sensitivity analysis. *Comput .&Struct .*, **64**(1 – 4): 31 – 63.

Wu, Q., 1997. Finite element analysis for laminated structure with visco-elastic layer. Doctor's Thesis, Zhejiang University (in Chinese).

Xu, X. and Ling, D.S., 2001. Degenerated solid elements. *ACTA MECHANICA SOLIDA SINICA*, *Special issue for computational mechanics*, **22**: 1 – 12 (in Chinese).

Zienkiewicz, O. C. and Campbell, J. S., 1973. Shape optimization and sequencial linear programming. In: *Optimization Structural Design*, John Wiley & Sons, London.